

Noise-Induced Spectral Shift Measured in a Double Quantum Dot

B. Küng,^{1,*} S. Gustavsson,¹ T. Choi,¹ I. Shorubalko,¹ T. Ihn,¹ S. Schön,² F. Hassler,³ G. Blatter,³ and K. Ensslin¹

¹*Solid State Physics Laboratory, ETH Zurich, 8093 Zurich, Switzerland*

²*FIRST Laboratory, ETH Zurich, 8093 Zurich, Switzerland*

³*Theoretische Physik, ETH Zurich, 8093 Zurich, Switzerland*

(Dated: April 23, 2009)

We measure the shot-noise of a quantum point-contact using a capacitively coupled InAs double quantum dot as an on-chip sensor. Our measurement signals are the (bidirectional) inter-dot electronic tunneling rates which are determined by means of time-resolved charge sensing. The detector frequency is set by the relative detuning of the energy levels in the two dots. For non-zero detuning, the noise in the quantum point-contact generates inelastic tunneling in the double dot and thus causes an increase of the interdot tunneling rate. Conservation of spectral weight in the dots implies that this increase must be compensated by a decrease of the rate close to zero detuning, which is quantitatively confirmed in our experiment.

PACS numbers: 73.63.Kv, 73.63.Nm, 72.70.+m, 73.23.Hk

Charge detection with on-chip sensors provides a powerful tool for investigating the electronic properties of mesoscopic circuits. By performing the detection with sufficient bandwidth, the observation of single-electron charging events in real-time becomes possible, which has been used, e.g., to read out the spin of quantum dots [1], to investigate the transport statistics of interacting electrons [2, 3], or to measure small currents [3, 4, 5]. One of the simplest detectors offering enough sensitivity to perform this kind of experiments is the quantum point-contact (QPC) [6]. However, the quantum dots (QDs) that are typically probed by QPC sensors represent highly sensitive electronic devices on their own. Charge detection therefore comes with a considerable amount of back-action of the QPC on the QD to which both photons [7, 8] and phonons [9, 10] have been shown to contribute.

One way of describing the photonic part of the back-action is in terms of the shot-noise of the QPC which couples capacitively to the QD system and generates photon-assisted tunneling (PAT) [11]. From this viewpoint, the QD system can serve as an intrinsically fast *measurement* device for the QPC noise [5, 12], in particular when using a double quantum dot (DQD) which allows for frequency-tunable noise detection via control of the inter-dot level detuning [7]. We present here an experiment of that kind on a sample well suited for the purpose, with the QPC fabricated in a different host crystal (GaAs/GaAlAs) than the noise probe (an InAs DQD), thus suppressing the phononic interaction that competes with the capacitive coupling. The capacitive coupling on the other hand is extraordinarily large, which manifests itself in QPC conductance changes exceeding 50% caused by dot charging, while the corresponding figure for topgate- or AFM-defined samples is typically a few percent [13, 14]. In contrast to previous experiments, we are able to measure the response of the DQD along the whole detuning axis from positive to negative values. In

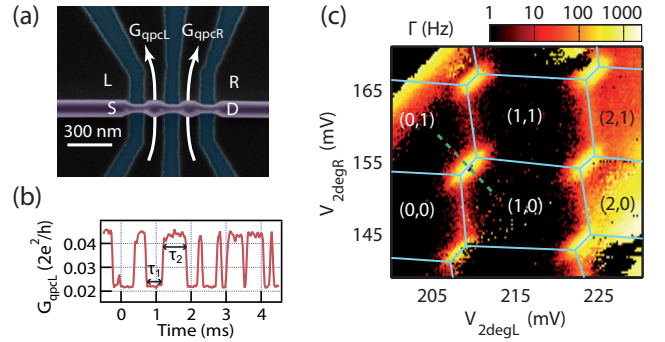


FIG. 1: (Color online) (a) SEM image of the device. A single etching step defines the DQD in the nanowire (horizontal) and constrictions in the 2DEG underneath. The white arrows indicate the direction of negative current through the point contacts. (b) Conductance G_{qpcL} of the left QPC measured time-resolved at a gate configuration where charge exchange between the dots is energetically allowed. The QPC conductance drops whenever an electron tunnels from the right into the left dot. (c) Charge stability diagram of the DQD obtained by evaluating the event rate $\Gamma = 1/(\tau_1 + \tau_2)$ in traces as in (b). The solid lines delineate regions of stable occupation numbers (n, m) of the DQD relative to $(0, 0)$. The subsequent measurements are carried out along the dashed line.

particular, we observe the reduction of the DQD tunneling rate around zero detuning in response to the QPC noise [11], an effect which is associated with the normalization of the spectral density of the dot wavefunctions.

Figure 1(a) shows a scanning electron microscope (SEM) image of the sample. It is fabricated by depositing an InAs nanowire on top of a GaAs/AlGaAs heterostructure containing a 37 nm deep two-dimensional electron gas (2DEG; density $4 \times 10^{11} \text{ cm}^{-2}$, mobility $3 \times 10^5 \text{ cm}^2/\text{Vs}$ at 2 K). By subsequent electron beam lithography and wet etching, QDs in the nanowire and constrictions in the 2DEG are defined simultaneously which ensures perfect alignment between QD and sensor

(for details see Refs. 15 and 16). The parts of the 2DEG marked ‘L’ and ‘R’ serve as side gates to tune the QPC conductances. Similarly, the QPCs are used as gates to selectively tune the QD potentials by applying offset voltages $V_{2\text{degL}}$, $V_{2\text{degR}}$ to both source and drain. All measurements were done in a ^4He cryostat at $T = 2\text{ K}$.

The DQD is operated at zero source-drain voltage and is tuned to a regime with very opaque barriers where its charge dynamics is monitored with the QPC sensors. These are biased with source-drain voltages V_{qpcL} , V_{qpcR} and their currents are measured with a bandwidth of 10 kHz. Figure 1(b) shows a typical time dependence of the left QPC’s conductance, which exhibits steps whenever a dot charging-event takes place. In measuring the event rate $\Gamma = 1/(\tau_1 + \tau_2)$ as a function of $V_{2\text{degL}}$ and $V_{2\text{degR}}$, we expect to reproduce the DQD charge stability diagram with nonzero Γ along the boundaries of the hexagonal regions of stable charge. In the corresponding graph in Fig. 1(c), which contains the data from the left QPC readout, we observe nearly vertical lines belonging to tunneling between the left QD and the source lead ($\sim 10\text{ Hz}$) and short, diagonal lines where inter-dot tunneling takes place ($\sim 1\text{ kHz}$). The horizontal charging lines of the right dot are only visible in the time-averaged signal (not shown), as the associated dot-drain transitions are too fast to be resolved in real time. Index pairs (n, m) mark the electron occupancy of the DQD in the corresponding hexagonal panel relative to the state $(0, 0)$. Apart from the features associated with the DQD, counts are detected in the $(2, 0)$ and $(2, 1)$ regions, as well as in the top left corner of the plot 1(c). These are caused by charge traps in the vicinity of the QPCs.

In moving along the dashed line in Fig. 1(c), we continuously vary the energy difference $\delta = \mu_R^1 - \mu_L^1$ between the charge configurations $(1, 0)$ and $(0, 1)$, as illustrated in the level diagram in Fig. 2(a). The energies μ_L^2 and μ_R^2 required for doubly occupying the DQD are higher by the mutual charging energy $E_m \approx 0.8\text{ meV}$, which was determined by finite-bias spectroscopy. An electron in the lower energy dot can tunnel to the higher energy dot by absorbing an energy quantum $|\delta|$ from the environment. The DQD system therefore acts as a tunable and frequency-selective probe for electrical noise in its vicinity [7, 11].

By applying a voltage $V_{\text{qpcL(R)}}$ across one of the QPCs, we generate broadband noise with a high-frequency cut-off at $eV_{\text{qpcL(R)}}/\hbar$, meaning that the electrons passing through the QPC have an exponentially small probability to emit photons with energies higher than the bias energy [7, 11, 17]. Due to the capacitive coupling, the generated photons can be absorbed by the DQD and drive inelastic transitions. In measuring the inter-dot tunneling rate Γ as a function of δ for increasing QPC bias, we therefore expect the equilibrium tunneling peak at $\delta = 0$ to become broadened due to photon absorption in a window $|\delta| < |eV_{\text{qpcL(R)}}|$. In Fig. 2(b), we plot the correspond-

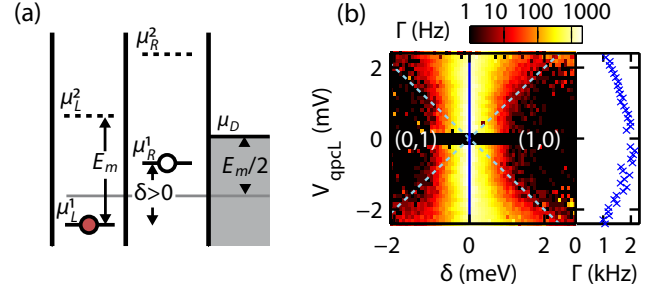


FIG. 2: (Color online) (a) Energy level diagram of the DQD system and the drain lead. Upon adding a second electron to the DQD, the levels μ_L^1 , μ_R^1 shift by the mutual charging energy E_m to the new positions μ_L^2 , μ_R^2 . (b) Grayscale (colourscale) plot of the inter-dot tunneling rate Γ as a function of level detuning δ [dashed line in Fig. 1(c) with $(\mu_L^1 + \mu_R^1)/2 = \mu_D - E_m/2$] and source-drain voltage V_{qpcL} across the left QPC. Photons with energies bounded by $|eV_{\text{qpcL}}|$ are emitted by the QPC and can drive inelastic tunneling events which leads to a broadening of the main peak (dashed lines indicate the condition $\delta = \pm eV_{\text{qpcL}}$). The plot on the right is a cut through $\delta = 0\text{ meV}$ (solid line).

ing measurement for bias applied across the left QPC. A small region $|V_{\text{qpcL}}| < 0.15\text{ mV}$, where the signal-to-noise ratio of the counting signal is not sufficient, is excluded from the data.

A remarkable feature of the data in Fig. 2(b) is the fact that not only the peak *width* is influenced by the QPCs, but also its *amplitude*. The maximum Γ at $V_{\text{qpcL}} = \pm 2\text{ mV}$ is smaller by a factor of 0.6 compared to the maximum at $V_{\text{qpcL}} \approx 0\text{ mV}$. Direct gating by the voltage V_{qpcL} can be excluded as the origin because of the magnitude of the effect, and secondly because of the symmetry in positive and negative V_{qpcL} . A similar reduction of the resonant current through a QD as a function of QPC bias, has been reported in Ref. 12. There, the effect could be explained by the excitation of an electron on the dot to a higher energy state, from where it had the chance to tunnel back to the source lead.

We propose that in our measurements dot-lead processes are not relevant; this will be justified in more detail later in this paper. Instead, the reduction of Γ at zero δ is directly linked to its increase at non-zero δ via shift of spectral weight. For the discussion of this effect, we consider the QPC as a source of voltage noise, i.e., potential fluctuations across the central dot barrier. Such fluctuations lead to inelastic tunneling through the central barrier, which is expressed in terms of the probability density for the dot to exchange energy quanta E with the source of the field [18],

$$P(E) = \frac{1}{2\pi\hbar} \int dt \exp[J(t) + iEt/\hbar]. \quad (1)$$

Here, the field is described in terms of the autocorrelation function $J(t) = \langle [\hat{\phi}(t) - \hat{\phi}(0)]\hat{\phi}(0) \rangle$ of the phase

operators $\hat{\phi}(t) = \int_0^t dt' e\hat{V}(t')/\hbar$. Equation (1) is valid for fields $\hat{V}(t)$ with typical frequencies much larger than the tunneling rate through the barrier, a regime in which $P(E)$ can be interpreted as the spectral density of the electronic state in either of the two dots. It is normalized to unity and determines the δ -dependence of the unidirectional tunneling rates between the dots, namely $\Gamma_{L\leftarrow R}(\delta) \equiv \Gamma_{LR}(\delta) \propto P(\delta)$ (right to left) and $\Gamma_{RL}(\delta) \propto P(-\delta)$ (left to right).

The voltage fluctuations across the two dots split into an *equilibrium* part $S_V^{(0)}(\omega)$, which includes thermal fluctuations in the nanowire (phonons [19]) as well as contributions from the QPC, and an *excess* part $S_V^{\text{ex}}(\omega, V_{\text{qpcL}})$, generated by the QPC at finite voltage V_{qpcL} . The equilibrium contribution determines the line shape of the rates $\Gamma_{RL/LR}$ at zero QPC voltage, while the finite-bias noise shifts weight to higher/lower energies. Since the exponents $J(t) = J^{(0)}(t) + J^{\text{ex}}(t)$ for the equilibrium and the excess noise contributions are additive, it follows from Eq. (1) that their probability densities $P^{\text{ex}}(E)$ and $P^{(0)}(E)$ have to be convolved to obtain the total $P(E)$. Identifying $P(\delta, V_{\text{qpcL}}) \propto \Gamma_{LR}(\delta, V_{\text{qpcL}})$ and $P^{(0)}(\lambda) \propto \Gamma_{LR}(\lambda, 0)$ (and likewise for Γ_{RL}), we can relate the rates at finite and zero bias,

$$\Gamma_{LR}(\delta, V_{\text{qpcL}}) = \int d\lambda \Gamma_{LR}(\lambda, 0) P^{\text{ex}}(\delta - \lambda, V_{\text{qpcL}}). \quad (2)$$

To leading order in J^{ex} , the probability density $P^{\text{ex}}(E, V_{\text{qpcL}})$ can be expressed [11] through $S_V^{\text{ex}}(\omega, V_{\text{qpcL}})$,

$$P^{\text{ex}}(E, V_{\text{qpcL}}) = \left[1 - \frac{e^2}{\hbar^2} \int d\omega \frac{S_V^{\text{ex}}(\omega, V_{\text{qpcL}})}{\omega^2} \right] \delta(E) + \frac{e^2}{\hbar} \frac{S_V^{\text{ex}}(E/\hbar, V_{\text{qpcL}})}{E^2}. \quad (3)$$

We assume S_V^{ex} to be proportional to the current shot-noise S_I^{ex} of the QPC, which amounts to assuming a frequency-independent trans-impedance Z_{tr} relating the two. The shot-noise is given by [11]

$$S_I^{\text{ex}}(\omega, V_{\text{qpcL}}) = \frac{4e^2}{\hbar} D(1-D) \left[\frac{\hbar\omega + eV_{\text{qpcL}}}{1 - e^{-(\hbar\omega + eV_{\text{qpcL}})/k_B T}} + \frac{\hbar\omega - eV_{\text{qpcL}}}{1 - e^{-(\hbar\omega - eV_{\text{qpcL}})/k_B T}} - \frac{2\hbar\omega}{1 - e^{-\hbar\omega/k_B T}} \right], \quad (4)$$

where $D = G_{\text{qpcL}}\hbar/(2e^2)$ is the transmission coefficient of the QPC. The noise spectrum (4) is even in ω and is characterized by a high-frequency cutoff $|\omega| < |eV_{\text{qpcL}}/\hbar|$ that is smeared by temperature.

In the top row of Fig. 3, we plot the measurements of Γ_{RL} and Γ_{LR} as functions of V_{qpcL} and δ . The rates have been extracted from traces as that shown in Fig. 1(b) by averaging the time the signal spends in the low- or high-current state, $\Gamma_{RL} \approx 1/\langle\tau_1\rangle$ and $\Gamma_{LR} \approx 1/\langle\tau_2\rangle$ [2]. Indeed they qualitatively exhibit the principal features

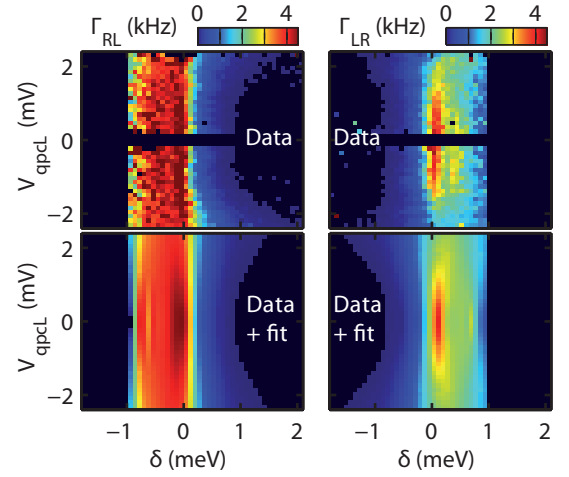


FIG. 3: (Color online) Top row: Grayscale (colorscale) plots of the unidirectional tunneling rates Γ_{LR} and Γ_{RL} as functions of detuning δ and QPC bias V_{qpcL} . Some of the data (Γ_{RL} : $\delta < -1$ meV; Γ_{LR} : $\delta > 1$ meV) with large statistical errors have been removed. Bottom row: Theoretical V_{qpcL} -dependence of the data reconstructed by numerical convolution of the measured cuts at $V_{\text{qpcL}} = -460 \mu\text{V}$ (ideally $V_{\text{qpcL}} = 0 \mu\text{V}$) with the spectral density $P^{\text{ex}}(E, V_{\text{qpcL}})$, Eq. (3).

expected from Eq. (3) combined with the spectrum (4), namely the reduction of their maxima around $\delta = 0$ and their increase on the excitation side of the δ axis (that is, $\delta > 0$ for Γ_{RL} , and $\delta < 0$ for Γ_{LR}).

For the quantitative comparison between experiment and theory, we simulated the effect of the QPC by numerically performing the convolution of the energy density (3) with the measured rates at a QPC bias close to zero. The only unknown parameter in this analysis is the trans-impedance Z_{tr} in $S_V^{\text{ex}}(\omega, V_{\text{qpcL}}) = |Z_{\text{tr}}|^2 S_I^{\text{ex}}(\omega, V_{\text{qpcL}})$ that was determined by minimizing the fitting error (weighted according to the inverse experimental uncertainty). Some care has to be taken concerning the coefficient D appearing in the noise spectrum (4). As seen in Fig. 1(b), the relative changes in G_{qpcL} caused by the hopping dot-electron are large and the D coefficient relevant for the $L \rightarrow R$ processes (corresponding to the low-current state of the QPC signal, $D_L = 0.021$) is therefore significantly different from the one relevant for $R \rightarrow L$ processes ($D_R = 0.045$). The result of the analysis is shown in the bottom row of Fig. 3, showing a good agreement between theory and experiment. Both data sets, $\Gamma_{LR}(\delta, V_{\text{qpcL}})$ and $\Gamma_{RL}(\delta, V_{\text{qpcL}})$, are best approximated using a trans-impedance of $Z_{\text{tr}} = 5.4 \text{ k}\Omega$. This value is roughly one order of magnitude larger than the corresponding figure given in Ref. 12, a fact which is well explained with the stronger capacitive coupling in the present case.

In order to rule out alternative explanations of the data, we shortly discuss how QPC-driven tunneling be-

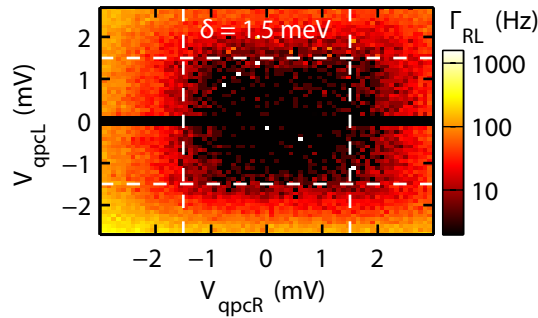


FIG. 4: (Color online) Photon absorption rate Γ_{RL} as a function of the left and right QPC source-drain voltages measured at fixed detuning $\delta = 1.5$ meV (dashed lines).

tween right dot and lead may affect the measurement of $\Gamma_{LR,RL}$. Including such tunneling processes, the rate $\Gamma_{LR}(\delta \approx 0 \text{ meV})$ would become smaller for increasing bias V_{qpcL} because an electron on the right dot may be excited into the lead (and tunnel back) instead of tunneling into the left dot. In the case of $\Gamma_{RL}(\delta \approx 0 \text{ meV})$ instead, the QPC may overcome the mutual charging energy and excite an electron from the lead into the right dot, thus blocking tunneling from left to right dot [see also Fig. 2(a)].

However, such dot-lead processes take place predominantly as compositions of excitations to an intermediate state and subsequent elastic tunneling into the lead (or, in the other direction, excitation of the valence electron of the dot and subsequent tunneling from the lead into the unoccupied low-energy state) [8]. This is in contradiction to the fact that there is no indication of an onset in bias voltage in the data, which should be present at the energy of the excited state, if dot-lead processes were relevant. Instead, the changes in $\Gamma_{RL,LR}$ are smooth and gradual, and already significant at eV_{qpcL} values below the typical single-particle excitation energy of 0.8 meV in our sample. Furthermore, we stress that the PAT theory is able to quantify the behavior of the rates on and off peak with a *single* parameter, whereas in a model incorporating dot-lead processes these two are separate regimes.

For all measurements presented up to now, the right QPC's source-drain voltage was set to zero. Similar to the left QPC, it is tuned to a low conductance of approximately $0.08 e^2/h$, and can be used as a noise source. This allows to test whether the perturbations created by the two QPCs have independent effects on the dot. Figure 4 shows a measurement of the tunneling rate Γ_{RL} at fixed detuning $\delta = 1.5$ meV (i.e., the photon absorption rate) as a function of left and right QPC bias voltages. The plot reveals a characteristic, square structure with a region of zero absorption in the inner part. This confirms the picture described above in the sense that there is a well-defined energy threshold for one-photon processes

($|eV_{qpcL}|, |eV_{qpcR}| > |\delta|$), and that to first order the effects of the two QPCs add independently. Two-photon processes with photons arriving at the double dot originating from the two QPCs would result in an additional, possibly diamond-like structure due to the differing energy conservation condition $|eV_{qpcL}| + |eV_{qpcR}| \geq |\delta|$. A measurement of the kind shown in Fig. 4 provides a unique way of directly mapping the addition of energies of photons [20] emitted by different sources.

We have investigated the process of photon-assisted tunneling driven by QPC noise in an InAs based DQD. Due to the full tunability of the DQD, we could observe the expected suppression of tunneling for zero dot detuning with increasing noise strength compensating for the increase in tunneling for nonzero detuning. Our data can be understood by treating the QPC as a classical, high-frequency noise source. Finally, by measurements with two separate emitter QPCs we confirm that their effects add up independently.

The authors thank F. Portier, G. Lesovik, and S. Ludwig for fruitful discussion. Financial support from the Swiss National Science Foundation (Schweizerischer Nationalfonds) is gratefully acknowledged.

* Electronic address: kuengb@phys.ethz.ch

- [1] J. M. Elzerman, R. Hanson, L. H. W. van Beveren, B. Witkamp, L. M. K. Vandersypen, and L. P. Kouwenhoven, *Nature (London)* **430**, 431 (2004).
- [2] S. Gustavsson, R. Leturcq, B. Simović, R. Schleser, T. Ihn, P. Studerus, K. Ensslin, D. C. Driscoll, and A. C. Gossard, *Phys. Rev. Lett.* **96**, 076605 (2006).
- [3] T. Fujisawa, T. Hayashi, R. Tomita, and Y. Hirayama, *Science* **312**, 1634 (2006).
- [4] J. Bylander, T. Duty, and P. Delsing, *Nature (London)* **434**, 361 (2005).
- [5] S. Gustavsson, I. Shorubalko, R. Leturcq, S. Schön, and K. Ensslin, *Appl. Phys. Lett.* **92**, 152101 (2008).
- [6] M. Field, C. G. Smith, M. Pepper, D. A. Ritchie, J. E. F. Frost, G. A. C. Jones, and D. G. Hasko, *Phys. Rev. Lett.* **70**, 1311 (1993).
- [7] S. Gustavsson, M. Studer, R. Leturcq, T. Ihn, K. Ensslin, D. C. Driscoll, and A. C. Gossard, *Phys. Rev. Lett.* **99**, 206804 (2007).
- [8] S. Gustavsson, I. Shorubalko, R. Leturcq, T. Ihn, K. Ensslin, and S. Schön, *Phys. Rev. B* **78**, 035324 (2008).
- [9] V. S. Khrapai, S. Ludwig, J. P. Kotthaus, H. P. Tranitz, and W. Wegscheider, *Phys. Rev. Lett.* **97**, 176803 (2006).
- [10] U. Gasser, S. Gustavsson, B. Küng, K. Ensslin, T. Ihn, D. C. Driscoll, and A. C. Gossard, *Phys. Rev. B* **79**, 035303 (2009).
- [11] R. Aguado and L. P. Kouwenhoven, *Phys. Rev. Lett.* **84**, 1986 (2000).
- [12] E. Onac, F. Balestro, L. H. W. van Beveren, U. Hartmann, Y. V. Nazarov, and L. P. Kouwenhoven, *Phys. Rev. Lett.* **96**, 176601 (2006).
- [13] L. M. K. Vandersypen, J. M. Elzerman, R. N. Schouten, L. H. W. van Beveren, R. Hanson, and L. P. Kouwen-

- hoven, Appl. Phys. Lett. **85**, 4394 (2004).
- [14] R. Schleser, E. Ruh, T. Ihn, K. Ensslin, D. C. Driscoll, and A. C. Gossard, Appl. Phys. Lett. **85**, 2005 (2004).
 - [15] I. Shorubalko, R. Leturcq, A. Pfund, D. Tyndall, R. Krschek, S. Schön, and K. Ensslin, Nano Lett. **8**, 382 (2008).
 - [16] T. Choi, I. Shorubalko, S. Gustavsson, S. Schön, and K. Ensslin, New J. Phys. **11**, 013005 (2009).
 - [17] E. Zakka-Bajjani, J. Ségala, F. Portier, P. Roche, D. C. Glatli, A. Cavanna, and Y. Jin, Phys. Rev. Lett. **99**, 236803 (2007).
 - [18] M. H. Devoret, D. Esteve, H. Grabert, G.-L. Ingold, H. Pothier, and C. Urbina, Phys. Rev. Lett. **64**, 1824 (1990).
 - [19] T. Fujisawa, T. H. Oosterkamp, W. G. van der Wiel, B. W. Broer, R. Aguado, S. Tarucha, and L. P. Kouwenhoven, Science **282**, 932 (1998).
 - [20] J. Tobiska, J. Danon, I. Snyman, and Y. V. Nazarov, Phys. Rev. Lett. **96**, 096801 (2006).